Kinetics of the RNA−DNA Helicase Activity of *Escherichia coli* Transcription Termination Factor Rho. 2. Processivity, ATP Consumption, and RNA Binding†

Katherine M. Walstrom, Jody M. Dozono, and Peter H. von Hippel*

Institute of Molecular Biology and Department of Chemistry, University of Oregon, Eugene, Oregon 97403

Received December 27, 1996; Revised Manuscript Received April 24, 1997⊗

ABSTRACT: The RNA-binding and RNA−DNA helicase activities of the *Escherichia coli* transcription termination factor rho have been investigated using natural RNA molecules that are 255 and 391 nucleotide residues in length and that contain the *trp t′* rho-dependent termination sequence of *E. coli*. Helicase substrates were prepared from these RNA molecules by annealing one or more DNA oligomers to complementary sequences located at or near the 3′-ends of the RNA molecules to form defined RNA−DNA hybrid sequences ranging in length from 20 to 100 bp. By comparing the fraction of the RNA molecules bound to rho with the fraction of bound DNA oligomers removed from the RNA during one round of the helicase reaction, we have shown that rho translocates processively at 37 °C in buffer containing 50 mM KCl. Helicase reactions and ATPase measurements were performed in parallel in the presence of RNA molecules containing RNA−DNA hybrids of various lengths, and we show that both the rate of translocation of the rho hexamer along the RNA chain and the rate of ATP consumption are similar, whether or not DNA is hybridized to the RNA transcript. By combining measurements of translocation and ATPase rates, we estimate that rho consumes ∼1−2 ATP molecules in translocating over 1 nucleotide residue of the RNA chain at 37 °C in 50 mM KCl. The ATPase activity of rho remains the same after one round of the helicase reaction, indicating that rho appears to hydrolyze ATP at the same rate, whether it is translocating along the RNA, separating RNA−DNA hybrids, or bound at the 3′-end of the RNA substrate. We also show that rho binds cooperatively (∼2−4 rho hexamers per RNA chain) to the RNA substrates under our standard helicase reaction conditions. However, cooperative binding is not essential for helicase activity, since this binding stoichiometry can be reduced to ∼1.5 rho hexamers per 255-nucleotide residue RNA chain by blocking ∼100 nt of either end of the rho binding site of the helicase substrate with complementary DNA oligonucleotides, with no change in helicase properties. The implications of these results for models of rho helicase function and for the role of rho in termination are discussed.

The participation of transcription termination protein rho is required to induce termination at about half of the termination sites of the *Escherichia coli* genome. The mechanism of this rho-dependent termination and ribonucleic acid (RNA)[1] release is not fully understood, but it has been speculated that rho may act, at least in part, as an ATP-driven (5′ → 3′) RNA-DNA helicase to separate the nascent RNA from the DNA transcription template, since rho has been shown to carry just such a helicase activity (*1, 2*). In the companion paper (*3*), we have characterized the kinetics of this RNA−DNA helicase activity and described the use of various rho- and DNA oligomer-trapping procedures to restrict the reaction to a single round of helicase activity. In addition, we showed that the rates of translocation of rho along the RNA component of the helicase substrate can be estimated from the rates of single-round helicase reactions. To reach the RNA polymerase complex effectively, the translocation of rho along the nascent RNA must also be quite processive. In this paper, we combine helicase activity measurements with rho−RNA binding studies to determine the processivity of translocation of rho along RNA.

All RNA and DNA helicases use the free energy released by ATP hydrolysis to fuel the protein conformational changes that allow the protein to translocate and to separate nucleic acid duplexes (reviewed in reference *4*). These reactions may be similar to those carried out by motor proteins, such as myosin and kinesin, which translocate directionally along actin filaments or microtubules (*5*). The efficiency of the coupling of the chemical free energy released from ATP hydrolysis to the reactions that result has been studied for only a few systems. For *E. coli* RecBCD, a helicase involved in DNA recombination and perhaps DNA repair, ∼2−3 ATP molecules are consumed in unwinding 1 bp of the double-stranded DNA substrate (*6*). Early experiments with the rho helicase reaction suggested that it hydrolyzes large amounts of ATP in discharging its helicase function; e.g., ∼4000 molecules of ATP appeared to be hydrolyzed in releasing a

† This research was supported in part by U.S. Public Health Service Research Grants GM-15792 and GM-29158 (to P. H.v.H.), by NIH Individual National Research Service Award GM-16069 (to K.M.W.), and by a grant to the Institute of Molecular Biology at the University of Oregon from the Lucille P. Markey Charitable Trust. P.H.v.H. is an American Cancer Society Research Professor of Chemistry.

* Corresponding author. Telephone: 541-346-5151. FAX:541-346-5891. E-mail: petevh@molbio.uoregon.edu.

⊗ Abstract published in *Advance ACS Abstracts,* June 15, 1997.

[1] Abbreviations: ATP, adenosine 5′-triphosphate; ATPase, adenosine-5′-triphosphate hydrolase; bp, base pair(s); DNA, deoxyribonucleic acid; DTT, dithiothreitol; EDTA, ethylenediaminetetraacetic acid; HEPES, *N*-(2-hydroxyethyl)piperazine-*N*′-2-ethanesulfonic acid; nt, nucleotide(s); OAc, acetate; P_i, inorganic phosphate; poly(dC), poly(deoxycytidylic acid); PEI, poly(ethylenimine); poly(rC), poly(cytidylic acid); rC, ribocytidine; rU, ribouridine; RNA, ribonucleic acid; TLC, thin-layer chromatography.

S0006-2960(96)03180-7 CCC: $14.00

single RNA−DNA hybrid from an ~250 nt RNA helicase substrate annealed to a complementary 28 nt DNA sequence (*2*). We report here the results of ATPase assays performed in parallel with helicase reactions that show that rho utilizes ATP much more efficiently than this in the actual process of releasing DNA from RNA−DNA hybrids.

It is known that rho binds cooperatively to polynucleotides, with a cooperativity parameter (ω) of ~400 (*7, 8*). As a consequence, it is important to determine the stoichiometry with which rho binds to the loading site of the helicase substrate in this study. Since rho functions as a hexamer (*9*−*11*), this value of ω means that a second rho hexamer has an ~400-fold greater probability (per unoccupied site) of binding next to a previously bound hexamer than of binding to an isolated site (see reference *12*). We show here that 2−4 rho hexamers bind to the RNA component of the helicase substrates under our standard helicase reaction conditions, presumably as a consequence of the cooperativity of rho binding and the large size of the *trp t′* rho loading site. This raises the question of whether more than one rho hexamer is required for helicase (and perhaps for termination) activity. We show here that one rho hexamer bound per loading site can suffice for helicase function.

MATERIALS AND METHODS

Figure 1 shows the RNA and DNA polynucleotides that were synthesized for these experiments. Rho protein, the polynucleotides poly(rC) and poly(dC), the RNA_{255} and RNA_{391} components of the helicase substrates, and the DNA oligomers used in these experiments were prepared, purified, and characterized as described in the companion paper (*3*). Additional DNA oligomers used in these experiments are shown in Figure 1. Helicase assays, gel electrophoresis, rho−RNA binding measurements, and data analysis were all performed as described in the companion paper (*3*).

ATPase Experiments. ATPase assays containing 10 nM RNA molecules and 10 nM rho hexamers were performed in 20 μL reactions in helicase buffer [20 mM HEPES (pH 7.9), 50 mM KCl, 1 mM $Mg(OAc)_2$, 0.1 mM EDTA, and 0.1 mM DTT]. The reactions also contained 0.7 μCi of [γ-^{32}P]ATP (3000 Ci/mmol, DuPont-NEN) and 1 mM unlabeled ATP. Rho was added to start the reactions. After various incubation times at 37 °C, 1 μL aliquots were removed from the reaction and spotted on a PEI−cellulose F TLC plate (EM Science) and developed with 0.35 M potassium phosphate (pH 7.5) buffer (*13*). The inorganic phosphate (P_i) and ATP spots were quantified in one of three ways: with an AMBIS radioanalytic scanner (Scanalytics), with a Molecular Dynamics Storm 860 Phosphorimager, or by cutting out the spots and quantitating them by liquid scintillation counting. Rates of ATP hydrolysis were determined by measuring the increase in the fraction of P_i (F_{P_i}, defined as $[P_i]/([P_i] + [ATP])$) in each sample. The rates were calculated using eq 1:

$$R = \left(\frac{\Delta F_{P_i}}{\Delta t}\right)[\mathrm{ATP}]\left(\frac{1}{[\mathrm{rho}]}\right) \qquad (1)$$

where $\Delta F_{Pi}/\Delta t$ is the slope of a plot of F_{Pi} vs time, [ATP] is the total initial ATP concentration, and [rho] is the concentration of rho hexamers.

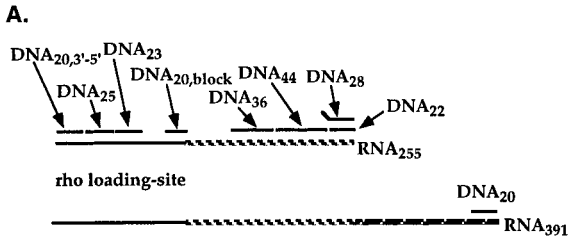

B.

DNA_{22}	gggatcctctagagtcgacact
$DNA_{20,3'-5'}$	gcatgcaagcttgagtattc
DNA_{44}	cattaaaattagtcgctaatgagaattagtcaaattaagcgcaa
DNA_{28}	gatcctctagagtcgacactttaatttt
DNA_{20}	ctggcgaaaggggatgtgc
DNA_{36}	cgagaagatagagggaaaatatattttgaggaacat
DNA_{25}	aaaaatgacgtaagttgacctgcag
DNA_{23}	ttgattatattactgttgggcgg
$DNA_{20,block}$	attgattttactggtgttat

FIGURE 1: RNA and DNA components of the helicase substrates used in these experiments. (A) The diagram shows where the DNA oligomers anneal to the RNA substrates. The long lines designate RNA, while the narrow sections designate the rho loading site. RNA segments with the same sequence are shown with the same shading pattern. The short lines, designating DNA, are shown next to the part of the RNA to which they anneal. The lengths of the lines are proportional to the lengths of the polynucleotides. The name of each molecule indicates its length and whether it is RNA or DNA. For example, DNA_{22} is a 22 nt DNA oligomer. The 20 nt DNA oligomers also include a descriptive name in the subscript to distinguish them from one another. The 3′-5′ subscript on $DNA_{20,3'-5'}$ denotes the direction of the helicase reaction required to remove it. The term "block" in the subscript for $DNA_{20,block}$ indicates that we used this oligomer to block rho binding. DNA_{22}, DNA_{44}, and DNA_{36} anneal next to one another. DNA_{28} contains 20 nt on the 5′-end that anneal to the 3′-end of RNA_{255}, while the remaining 8 nt on the 3′-end are completely noncomplementary to RNA_{255}. $DNA_{20,3'-5'}$, DNA_{25}, and DNA_{23} anneal next to one another. DNA_{23} and $DNA_{20,block}$ anneal 18 nt apart, and $DNA_{20,block}$ and DNA_{36} anneal 49 nt apart on the RNA. The RNA substrate is described in detail in Walstrom et al. (*3*). The corresponding trapping DNA oligomers were all 16−20 nt in length and have sequences complementary to each DNA oligomer that anneals to the RNA. For the longer DNA oligomers, two short trapping oligomers were used instead of one long oligomer. (See reference *3* for a description of the use of the trapping DNA oligomers.) In Figures 3 and 5, simpler versions of this figure are shown in small diagrams indicating the helicase substrate used in each experiment. (B) Sequences of the DNA oligomers used in these experiments, shown in 5′ → 3′ orientation.

RESULTS

In the companion paper (*3*), we have shown that single-round rho helicase reactions can be isolated and measured. Such single-round reactions correspond to a pre-steady-state burst of activity, and the rate constant of this fast phase of the helicase kinetics can be used to estimate the translocation rate of rho along the RNA of the helicase substrate. In this paper, we describe experiments that address the following questions: (i) How processively does rho translocate along an RNA molecule that contains a rho loading site? (ii) Does the concomitant ATPase reaction have a burst phase? (iii) Does rho translocate more rapidly (or more slowly) along single-stranded RNA than it does through an RNA−DNA hybrid? (iv) Does rho hydrolyze the same amount of ATP per nucleotide residue traversed while translocating along single-stranded RNA as it does in unwinding an RNA−DNA

Table 1: Processivity of the Rho Helicase Reaction[a]

rho hexamers (nM)	RNA substrate[b]	[rho]/ [RNA]	fraction of RNA bound to rho[c]	amplitude of helicase burst phase[d]
5	RNA_{255}	0.5	0.19 ± 0.01	0.17 ± 0.04
10	RNA_{255}	1	0.42 ± 0.04	0.41 ± 0.03
20	RNA_{255}	2	0.6 ± 0.1	0.73 ± 0.03
10	RNA_{391}	1	0.26 ± 0.07	0.27 ± 0.05
20	RNA_{391}	2	0.5 ± 0.1	0.57 ± 0.05

[a] Reactions were performed in helicase buffer containing 50 mM KCl and the indicated rho and RNA concentrations. [b] Either RNA_{255} or RNA_{391} alone or RNA_{255}/DNA_{22} or RNA_{391}/DNA_{20} were used for the filter-binding measurements. [c] Determined using nitrocellulose filter-binding measurements at 22 °C in the presence of 1 mM ATP. The trapping DNA oligomers (see reference *3*) do not affect the rho−RNA binding results (data not shown). There was no significant difference in the measurements obtained with RNA alone or with the annealed substrates (data not shown). The listed errors correspond to the standard deviation of the measurements. [d] Determined using helicase assays at 37 °C as described in Walstrom et al. (*3*). The listed errors correspond to errors from fitting data to eq 1 in Walstrom et al. (*3*).

hybrid? (v) How many rho hexamers are bound to each RNA molecule in the helicase reaction under various conditions?

ATP-Driven Rho Translocation Is Processive from the Rho Loading Site to the 3′-End of the RNA. The methods of the previous paper (*3*) can be used to determine the fraction of complementary DNA oligonucleotides removed from the RNA substrate in a single-round helicase reaction at different rho to RNA concentration ratios and with different RNA substrates. These results are summarized in Table 1 and can be compared to the fraction of RNA molecules bound to rho as measured using the nitrocellulose filter-binding assay under the same reaction conditions (see Table 1). The results show that a similar fraction of the total RNA_{255}/DNA_{22} substrate is initially bound to rho in the presence of ATP and releases a DNA_{22} oligomer during one round of the helicase reaction in 50 mM KCl at 37 °C (Table 1). The same result was demonstrated for the RNA_{391}/DNA_{20} substrate. These findings show that rho translocates along the RNA processively under these assay conditions, because each helicase substrate that was originally bound to rho releases a DNA oligomer in a single-round reaction.

ATP was added to the binding reactions shown in Table 1 to simulate the actual conditions of the helicase reaction more closely. ATP was added less than 1 min before the solutions were filtered, so that very little was hydrolyzed prior to filtration. In the preceding paper (*3*), we showed that in contrast to the complementary DNA, rho is released from RNA_{255} very slowly, both in the presence and in the absence of ATP. This means that a similar amount of rho was bound to RNA both before and after the addition of ATP, since the rate of dissociation of rho from the RNA was too slow to permit recycling to another helicase substrate molecule after ATP addition, but before filtration. We confirmed this directly with binding experiments in the absence of ATP (data not shown). In addition, the fraction of RNA_{255} molecules bound to rho in the presence of ATP was the same, whether the RNA was annealed to the DNA oligomer or not (data not shown). This is consistent with the hypothesis that rho binds initially to the RNA at the rho loading site, which is located at the opposite end of the RNA molecule from the RNA−DNA hybrid (see Figure 1). We have used such rho−RNA binding measurements to determine the stoichiometry of rho binding to the RNA of the helicase substrate (see below and Table 2).

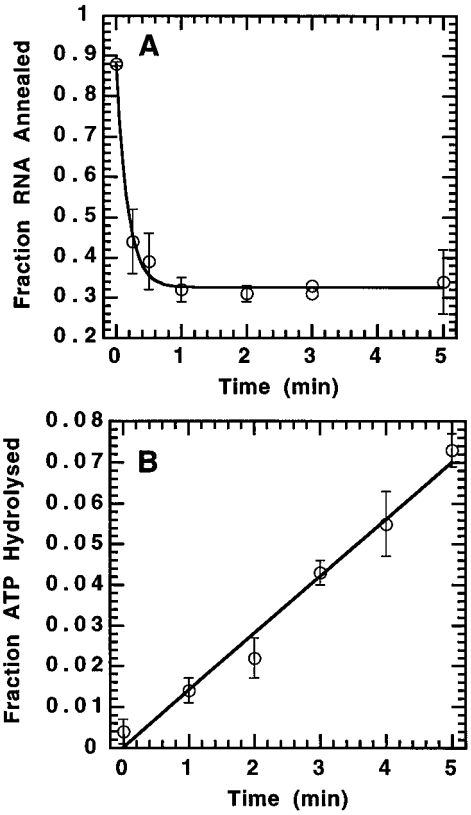

FIGURE 2: Helicase and ATPase reactions under the same reaction conditions. (A) Helicase reactions were performed in helicase buffer at 37 °C with 10 nM RNA_{255}/DNA_{44} hybrids and 10 nM rho hexamers in the presence of 3 μM poly(rC), as described under Materials and Methods. The fraction of RNA_{255} annealed to DNA_{44} was determined at each time point. The data were fit to the following equation: $y = A_1e^{-(k_1t)} + A_2$, where A_1 and A_2 are the amplitudes of the two components and k_1 is the rate constant of decay of the exponential component. The results of the fit are $A_1 = 0.55$ (± 0.02) and $k_1 = 6$ (± 1) min^{-1}. Each data point represents the average of 3−4 measurements, and the error bars show the standard deviation. (B) ATPase assays were performed with 10 nM RNA_{255}/DNA_{44} hybrids and 10 nM rho hexamers in helicase buffer at 37 °C, as described under Materials and Methods. Note that these samples do not contain poly(rC) (see Results for a discussion). The fraction of ATP hydrolyzed to radioactive P_i was determined at each time point. The ATPase activity [23 (± 2) ATP molecules hydrolyzed per rho hexamer per second] was determined from the slope of a straight line passed through the data (eq 1) using a least-squares fit. Each symbol represents the average of 3−4 measurements, and the error bars correspond to one standard deviation.

The Rho−ATPase Reaction Does Not Show a Burst Phase. In the companion paper, we showed that the helicase reaction in 50 mM KCl proceeds in two phases: (i) a rapid burst phase that reflects the first round of the helicase reaction; and (ii) a slow phase that reflects a complex combination of secondary and rho rebinding reactions (reference *3* and Figure 2A). In contrast, we show in Figure 2B that the ATPase activity of rho is linear over the entire time course of the helicase reaction. In other experiments, we measured the ATPase activity of rho at 15 s intervals during the first minute of the reaction and observed the same linear rate (data not shown). This shows that the ATPase activity of rho is the same while translocating along the RNA, while unwinding the RNA−DNA hybrid (i.e., during the first phase of the helicase reaction), while bound to the RNA substrate after translocation has been completed (i.e., during the second

phase of the reaction), and after releasing the first RNA substrate and binding a new one. The implications of this result for the operation of the ATP-driven RNA binding and release cycle within the rho hexamer are considered under Discussion. The specific ATPase rates shown in Figures 2B and 3B were calculated using the total rho concentration. We show below that all of the rho hexamers are bound to RNA under our reaction conditions.

The helicase reactions shown in Figures 2A and 3A were performed in the presence of a poly(rC) trap to restrict the reaction to a single round (see reference *3*). The parallel ATPase reactions were performed in the absence of poly(rC). We showed in the preceding paper (*3*) that rho releases the RNA substrate slowly after the first round for assays carried out in 50 mM KCl-containing buffer. Therefore, in these experiments, most of the rho remains bound to the helicase substrate even in the presence of the poly(rC) trap. ATPase assays performed in the presence or absence of poly(rC) or poly(dC) give the same ATPase activity for the first 3−4 min of the reaction (data not shown), indicating that the transfer of rho from the helicase substrate to the rho trap is slow. We performed some experiments in which we removed samples for helicase and ATPase measurements from the same solution and obtained similar results (data not shown).

Rho Translocates along Single-Stranded RNA at Least as Fast as It Moves through the RNA−DNA Hybrid. We performed helicase measurements with RNA_{255} annealed to multiple DNA oligomers, as shown in Figure 1, to compare the rate of translocation of rho along single-stranded RNA to the rate of translocation through an RNA−DNA hybrid. The DNA oligomers used were bound to RNA_{255} to form RNA−DNA hybrids (at the 3′-end of the RNA) that ranged in length from 20 to 64 bp. The rates of the first phase of the helicase reactions with the different hybrid lengths were all similar to one another (Figure 3A) and to the rates measured for the RNA_{255}/DNA_{22} substrate at 10 and 20 nM rho concentrations (see reference *3*, and the open squares in Figure 3A). This indicates that moving through the RNA−DNA hybrids does not slow the translocation of rho along the RNA compared to the translocation rate over single-stranded regions. This appears to be true even for the longest hybrid examined (64 bp), which covers most of the length of the RNA that rho traverses during the helicase reaction (see below).

As the RNA−DNA hybrid on the helicase substrate becomes longer, the 5′-end of the hybrid moves closer to the loading site. We have shown that the rate constant of the first phase of the helicase reaction represents the translocation of rho along RNA and that the rate constant of DNA release from the RNA decreases as the distance between the rho loading site and the RNA−DNA hybrid becomes longer (*3*). Therefore, we expected that a DNA oligomer annealed closer to the rho loading site (DNA_{44}) would be released faster than a downstream oligomer (DNA_{22}); however, similar helicase rates were observed for all the helicase substrates under these conditions (Figure 3A). Note that the earliest time points in the experiments shown in Figure 3A were taken at 10 s, since we found that earlier time points could not be reliably measured by hand. As a result, the rates that we have determined here correspond to a minimum rate of translocation, since the burst phase of the reaction is almost complete in 10 s. To slow the reaction,

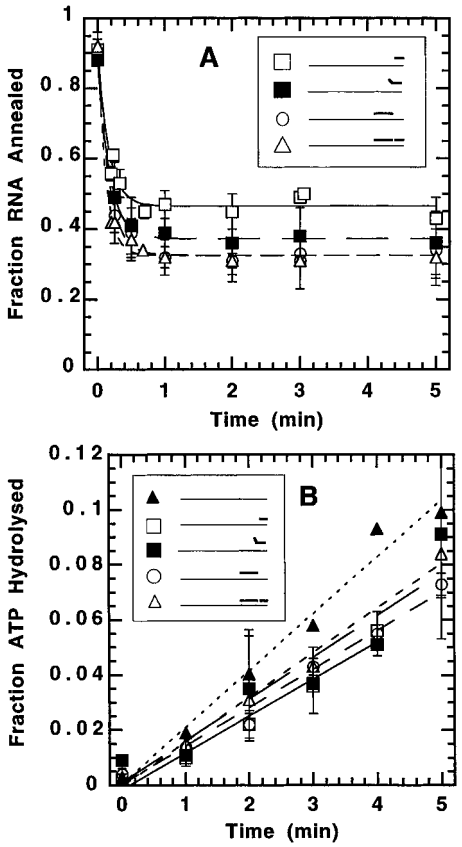

FIGURE 3: Helicase reactions with different lengths of RNA−DNA hybrid. (A) Helicase reactions were performed in helicase buffer at 37 °C, as described under Materials and Methods, with 10 nM rho hexamers in the presence of 3 μM poly(rC) and 10 nM of the following substrates: RNA_{255}/DNA_{22} (open squares), RNA_{255}/DNA_{28} (solid squares), RNA_{255}/DNA_{44} (open circles), and RNA_{255}/DNA_{44}-DNA_{22} (open triangles). The figure inserts show schematic views of the helicase substrates that are comparable to those shown in Figure 1A. The long thin line designates RNA, and the short thicker lines designate DNA. The fraction of RNA_{255} annealed to DNA was determined at each time point. The data were fit to the following equation: $y = A_1e^{-(k_1t)} + A_2$, where A_1 and A_2 are the amplitudes of the two components and k_1 is the rate constant of decay of the exponential component. The results of the fit for A_1 and k_1 (units in min^{-1}) for the different reactions are as follows: 0.43 (±0.04) and 7 (±2) (open squares, solid line); 0.51 (±0.02) and 6 (±1) (solid squares, long-dashed line); 0.55 (±0.02) and 6 (±1) (open circles, medium-dashed line); and 0.59 (±0.02) and 8 (±1) (open triangles, short-dashed line). Note that the last two lines overlap between 1 and 5 min. Each data point with error bars represents the average of 3−4 measurements, and the error bars correspond to the standard deviation. Individual symbols represent single measurements. The data points shown as open circles are also present in Figure 2A. (B) ATPase assays were performed in helicase buffer at 37 °C, as described under Materials and Methods, using 10 nM rho hexamers in the presence of the following substrates: RNA_{255} (solid triangles), RNA_{255}/DNA_{22} (open squares), RNA_{255}/DNA_{28} (solid squares), RNA_{255}/DNA_{44} (open circles), and RNA_{255}/DNA_{44}-DNA_{22} (open triangles). (The same symbols are used as in Figure 3A.) Note that these samples do not contain poly(rC) (see Results). The fraction of ATP hydrolyzed to P_i was determined at each time point. The ATPase activity of each sample was determined from the slope of a straight line passing through the data (eq 1) using a least-squares fit. The slopes of each line (in units of ATP molecules hydrolyzed per rho hexamer per second) are as follows: 34 ± 5 (solid triangles, dotted line); 22 ± 2 (open squares, solid line); 25 ± 6 (solid squares, long-dashed line); 23 ± 2 (open circles, medium-dashed line); and 27 ± 2 (open triangles, short-dashed line). Each symbol with error bars represents the average of 3−6 measurements. Individual symbols correspond to the average value of two different measurements. The data points represented by the open circles are also shown in Figure 2B.

Table 2: Stoichiometry of Rho Binding to RNA_{255} and RNA_{391}[a]

rho hexamers (nM)	RNA	[rho]:RNA ratio	RNA bound to rho (nM)[b]	rho hexamers per RNA[c]
5	RNA_{255}	0.5	1.9 ± 0.1	2.6 ± 0.2
10	RNA_{255}	1	4.2 ± 0.4	2.4 ± 0.2
20	RNA_{255}	2	6 ± 1	3.3 ± 0.6
10	RNA_{391}	1	2.6 ± 0.7	4 ± 1
20	RNA_{391}	2	5 ± 1	4.0 ± 0.8

[a] Reactions were performed in helicase buffer containing 50 mM KCl, 10 nM RNA, and the indicated concentrations of rho hexamers. [b] Calculated from the nitrocellulose filter-binding measurements shown in Table 1 and the total RNA concentration. [c] Calculated from columns 1 and 4. The Results describe experiments indicating that all of the rho hexamers are bound to RNA in these experiments. The listed errors correspond to the standard deviation for each set of measurements.

some helicase reactions were performed at lower temperatures. Under these conditions, the first (burst) phase was slower and showed, as expected, that the upstream oligomers appeared to be removed more rapidly than those located further downstream (Figure 5B). No intermediate RNA bands were observed in helicase reactions that monitored the removal of the contiguous DNA_{36}, DNA_{44}, and DNA_{22} oligomers from RNA_{255} (data not shown), indicating that these contiguous oligomers were still released essentially simultaneously on the time scale of our measurements (see further discussion below). We note that as the RNA−DNA hybrid on the RNA_{255} becomes longer, the amplitude of the first phase increases (Figure 3A). This reflects a redistribution of rho hexamers on the RNA substrates, as discussed in detail below.

Figure 3A also shows the results of helicase reactions performed with RNA_{255}/DNA_{28}, where DNA_{28} forms the same 20 bp RNA−DNA hybrid with RNA_{255} as does DNA_{22}, but carries an additional 8 nt on the 3′-end of the DNA oligomer that do not hybridize to the RNA (see Figure 1). The binding of this DNA oligomer creates a "forked" helicase substrate, which more closely resembles the forked RNA−DNA hybrid that is expected to occur within an elongating transcription complex. Figure 3A shows that the helicase reaction with this substrate proceeds at a similar rate to that seen with RNA_{255}/DNA_{22}, indicating that rho can remove a forked and a completely annealed DNA oligomer from RNA with equal facility.

Rho Hydrolyzes ATP at the Same Rate, Whether Translocating along Single-Stranded RNA or Displacing a DNA Oligomer from an RNA−DNA Hybrid. Similar specific ATPase activities were measured for rho in reactions with "bare" RNA_{255} and with helicase substrates carrying RNA−DNA hybrids ranging from 20 to 64 bp in length (Figure 3B). ATPase activity in the presence of the forked RNA_{255}/DNA_{28} substrate was also similar (Figure 3B), and the presence of trapping DNA oligomers (see reference *3*) did not affect the ATPase activity of rho (data not shown). We conclude that the specific ATPase activity of rho is the same, whether the protein is translocating along (or bound to) bare RNA or working as an RNA−DNA helicase. This result will be used to calculate the rate of ATP consumption by rho while it translocates along the RNA (see below).

Two to Four Rho Hexamers Are Bound to the RNA during the Helicase Reaction. The helicase and rho−RNA binding results presented in Table 2 indicate that there are 2−3 rho hexamers bound to each RNA_{255} chain of the helicase substrate, and ∼4 rho hexamers bound to each RNA_{391} chain, because the fraction of RNA molecules bound to rho was approximately half (for the RNA_{255} substrate) and one-fourth (for the RNA_{391} substrate) of the ratio of the RNA to rho hexamer concentrations, respectively. If multiple rho hexamers bind to each RNA substrate, there should be few unbound rho hexamers present in the rho−RNA mixtures. This was confirmed using the two different methods described below.

The fraction of free rho hexamers present in the helicase reactions could be estimated directly by taking advantage of the slow dissociation rate of RNA from rho (see reference *3*); in essence, the experiment involved adding a helicase reaction mixture to a solution of ATP plus poly(rC) and measuring the ATPase activity of the final mixture. Any unbound rho hexamers in the original solution would bind rapidly to the poly(rC) trap under these conditions and hydrolyze ATP at the higher specific rate that is characteristic of this cofactor. Rho hexamers bound to an RNA molecule (i.e., RNA_{255} or RNA_{391}) in the first solution would remain bound to that RNA molecule and would thus hydrolyze ATP at a lower rate. Using this procedure we have confirmed (data not shown) that essentially all of the rho hexamers are bound to the RNA substrate in the helicase reactions.

We also looked for conditions where fewer rho hexamers bound to each RNA substrate. At 0.2 nM rho hexamers and 0.2 nM RNA_{255}, 73 (±2)% of the RNA_{255} was bound to rho, suggesting that most of the RNA substrate only bound to one rho hexamer. Under these conditions, the specific ATPase activity of rho was 27 ± 8 ATP per rho hexamer per second, which is the same ATPase activity observed with 2 or 3 rho hexamers bound per RNA (Figure 3B). This indicates that the specific ATPase activity of rho is the same over a 50-fold concentration range, that all of the rho hexamers are bound to RNA under the helicase reaction conditions, and that cooperative binding of rho hexamers does not change the ATPase activity (see below).

One Rho Hexamer Can Separate an RNA−DNA Hybrid, but May Not Show Full Processivity in Translocating along Single-Stranded RNA. Since our results (above) show that more than one rho hexamer binds to the rho loading sites of our helicase substrates, we asked whether more than one rho hexamer is required to catalyze the full RNA−DNA helicase activity. We showed above that at 0.2 nM concentrations of rho hexamers and RNA_{255}, 73 (±2)% of RNA_{255} is bound to rho, indicating that ∼1.4 rho hexamers are bound per RNA_{255} molecule in the absence of ATP. We have shown that the presence of ATP does not change the rho−RNA binding (see above). When we performed helicase experiments at low rho and RNA concentrations, but in the presence of 1 mM ATP, only 30% of the RNA−DNA hybrids were separated in a single round (Figure 4). This shows that only half of the bound RNA molecules contained processive, active rho complexes and suggests that two rho hexamers may be required to processively translocate along single-stranded RNA to reach a downstream RNA−DNA hybrid. We did controls to show that the rho hexamers did not fall apart at these low concentrations before we performed the experiments (data not shown).

Another way to decrease the number of rho hexamers that can be loaded onto the RNA might be to decrease the length of the rho loading site on the helicase substrate. This was achieved by binding DNA oligomers to either end of the single-stranded rho loading site of the RNA of the helicase

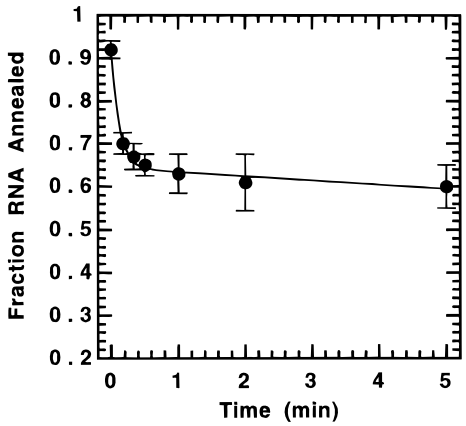

FIGURE 4: Helicase reaction at low rho and RNA concentrations. Helicase reactions were performed in helicase buffer at 37 °C, as described under Materials and Methods, with 0.2 nM rho hexamers and 0.2 nM RNA_{255}/DNA_{22}. The fraction of RNA_{255} annealed to DNA was determined at each time point. The data were fit to the following equation: $y = A_1e^{-(k_1t)} + (A_2 - k_2)$, where A_1 is the amplitude and k_1 is the rate constant of decay of the exponential component and A_2 and k_2 are the intercept and slope, respectively, of the linear component. The results of the fit for A_1 and k_1 are 0.28 (±0.02) and 8 (±1) min^{-1}, respectively. Each data point shows the average of three measurements, and the error bars correspond to the standard deviation. The fraction of RNA bound to rho under the same conditions (but in the absence of ATP) is 73 (±2)%.

substrate, thus effectively shortening the portion of the loading site to which rho can bind (see Figure 1), since rho does not bind to RNA−DNA hybrids (*14*−*16*). When we performed helicase assays with these partially blocked helicase substrates, we found that the amplitude of the burst phase was increased, indicating that a greater fraction of DNA oligomers were removed in a single round by rho (Figure 5A).

We found that only half of the DNA oligomers were removed in the burst phase of the helicase reaction (Table 1) in experiments with equal concentrations of RNA_{255}/DNA_{22} and rho hexamers. In the previous section, we showed that essentially all of the rho hexamers present are bound to RNA. Thus, ~2 rho hexamers are bound to each RNA_{255} substrate (see Table 2). The burst amplitudes for the reactions with the longer RNA−DNA hybrids are larger (Figure 5), and these experiments were performed under the same reaction conditions. This indicates that more of the RNA substrates were bound to rho and thus that fewer rho hexamers were bound per RNA substrate in these reactions. This was confirmed by RNA binding measurements that show that a larger fraction of RNA helicase substrates containing long RNA−DNA hybrids are bound to rho (data not shown). In effect, these experiments comprise a continuation of those shown in Figure 3A, which demonstrated that the amplitude of the helicase reaction increases with increasing RNA−DNA hybrid length. This indicates that the binding of a 64 nt DNA oligomer to the loading zone starts to inhibit the binding of a second rho hexamer to the helicase substrate (Figure 3A). The effect is even greater for a 100 bp hybrid (Figure 5A). Thus, only one rho hexamer per RNA chain is needed to drive the helicase reaction when rho loads on the RNA substrate near the RNA−DNA hybrid.

We blocked the RNA_{255} component of the helicase substrate at either end in these experiments to test whether the change in the reaction was caused by blocking the single-stranded region of the RNA substrate or by a change in the

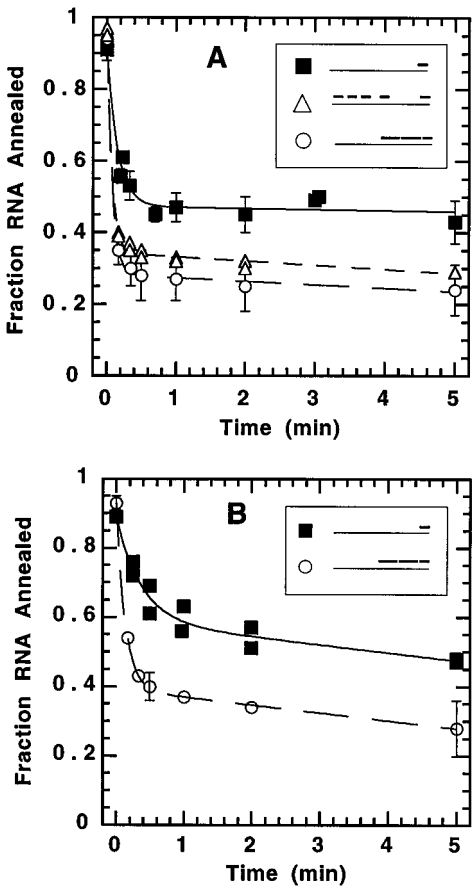

FIGURE 5: Helicase experiments with blocked RNA substrates. Helicase reactions were performed as described under Materials and Methods in helicase buffer with 10 nM RNA substrates and 10 nM rho hexamers at 37 °C in the presence of 3 μM poly(dC) (A) or at 22 °C in the absence of poly(dC) (B) with the following substrates: RNA_{255}/DNA_{36}-DNA_{44}-DNA_{22} (open circles); $RNA_{255}/DNA_{20,3'-5'}$-DNA_{25}-DNA_{23}-$DNA_{20,block}$-DNA_{22} (open triangles); or RNA_{255}/DNA_{22} (solid squares). The fraction of RNA_{255} annealed to all DNA oligomers was determined at each time point. Note that only DNA_{22} is removed by rho for the substrate shown in open triangles. The data were fit to the following equation: $y = A_1e^{-(k_1t)} + (A_2 - k_2t)$, where A_1 and k_1 are the amplitude and rate constant, respectively, of the exponential component and A_2 and k_2 are the y-intercept and slope, respectively, of the linear component [$k_2 = 0$ in the presence of poly(dC)]. The results of the fit for A_1 and k_1 (min^{-1}) for the different reactions are as follows: (A) 0.43 (±0.04) and 7 (±2) (solid squares, solid line); 0.61 (±0.01) and 14 (±1) (open triangles, medium-dashed line); 0.66 (±0.01) and 13 (±1) (open circles, long-dashed line); (B) 0.35 (±0.03) and 1.9 (±0.4) (solid squares, solid line); and 0.54 (±0.01) and 7.4 (±0.3) (open circles, long-dashed line). Symbols with error bars represent the average of 3−5 measurements, and the error bars correspond to one standard deviation. Individual symbols represent single measurements. The data points shown as solid squares in panel A are also shown in Figures 2 and 3 of (*3*).

properties of rho in the presence of a longer RNA−DNA hybrid. We showed in the preceding paper that rho is over 1000-fold more active as a 5′ → 3′ helicase than as a 3′ → 5′ helicase (*3*). This means that only DNA_{22} is removed during the helicase reaction for an RNA_{255} substrate blocked on the 5′-end, while all three DNA oligomers are removed when RNA_{255} is blocked on the 3′-end (Figure 5A). Note that the rho loading site of the substrate that is blocked at the 5′-end is largely occluded. Rho does not bind to this substrate as tightly as it does to the "open" rho loading site (data not shown). We suspect that rho can still use this blocked substrate because it does not have to translocate very

far to remove the DNA_{22} oligomer and because the 3′-end of the RNA_{255} molecule contains little RNA secondary structure (see Figure 1, reference *3*).

The Rate Constant of the Burst Phase Gives a Measure of the Rate of Rho Translocation. Since the burst phase of the helicase reaction is fast with the blocked substrates, we did not observe much of an increase in the rate constant of the burst phase as the upstream end of the RNA−DNA hybrid was moved closer to where rho binds to the RNA. In order to test again whether the rate constant of the burst phase of the helicase reaction gives a measure of the rate of rho translocation along the RNA (*3*), we performed experiments at 22 °C to slow down the helicase reaction (Figure 5B). We found that the substrate with the longer RNA−DNA hybrid was separated more rapidly than the short hybrid, suggesting that it takes longer for rho to reach a DNA oligomer that is annealed further away from the loading site. The amplitude of the RNA_{255}/DNA_{22} helicase reaction is smaller at 22 °C than at 37 °C, perhaps because the presence and stability of RNA secondary structure increase at lower temperatures and thus may affect the processivity of rho translocation along the RNA (K.M.W., unpublished results).

The Specific ATPase Activity of Each Rho Hexamer Bound to the RNA Helicase Substrate Is the Same. We measured the ATPase rate of rho in the presence of helicase substrates carrying partially blocked rho loading sites to determine unambiguously whether a rho hexamer hydrolyzes ATP at the same rate when it is bound to RNA alone and when it is bound to RNA next to a second rho hexamer. For RNA_{255} containing an ∼106 bp hybrid located on the 5′ side of the rho loading site, the ATPase activity [16 (±1) ATP molecules hydrolyzed per rho hexamer per second] is low, presumably because most of the rho loading site is blocked. The ATPase activity in the presence of RNA_{255} blocked by a 100-base hybrid on the 3′ side of the loading site [27 (±2) nM ATP molecules hydrolyzed per rho hexamer per second] is similar to the ATPase activity in the presence of the other RNA−DNA hybrids (Figure 3B). Since the specific ATPase activity is essentially unchanged when either ∼1 or ∼2 rho hexamers bind to each RNA helicase substrate at the rho loading site, this experiment confirms that each rho hexamer does indeed hydrolyze ATP at about the same rate.

One to two ATP molecules are hydrolyzed per rho hexamer in translocating over one RNA residue. In Figure 3B, we presented the ATPase rates for rho in 50 mM KCl in the presence of various helicase substrates containing RNA_{255}. The average rate observed was 26 (±5) ATP molecules hydrolyzed per rho hexamer per second. We also measured an ATPase rate of 41 (±2) ATP molecules hydrolyzed per rho hexamer per second in the presence of RNA_{391} (data not shown). In the previous paper, we showed that rho traverses over RNA at ∼20 RNA residues per second at 37 °C (*3*). By combining these results, we can estimate the rate of consumption of ATP by rho during the helicase reaction. If we assume that each rho hexamer translocates across each RNA residue of the helicase substrate, then this rate is ∼1 ATP molecule hydrolyzed per rho hexamer for every nucleotide residue of RNA traversed on RNA_{255} in 50 mM KCl at 37 °C, and ∼2 ATP molecules hydrolyzed per rho hexamer for every RNA nucleotide residue traversed on RNA_{391} under the same conditions.

DISCUSSION

In this paper, we present results from rho−RNA binding and ATPase measurements that were performed in parallel with the RNA−DNA helicase experiments described in the companion paper (*3*). We address additional questions regarding the translocation of rho along RNA, including its processivity and rate of ATP consumption per RNA nucleotide residue traversed. In addition, we show that rho binds cooperatively to the rho loading site in the helicase reactions, and that single rho hexamers bound to RNA have the same ATPase properties as rho hexamers bound cooperatively.

Processivity. In the previous paper, we discussed the rate of translocation of rho along the RNA substrate and showed that the rate we estimated is slower than the rate of transcript elongation by the RNA polymerase. In this paper, we have measured rho−RNA binding under the same reaction conditions and found that rho translocates processively along both RNA_{255} and RNA_{391} (Table 1). This indicates that rho can translocate for at least 300 nt along the nascent RNA when the reaction is performed in 50 mM KCl. Since many known rho-dependent termination sites are located less than 100 nt downstream of the rho loading site on the nascent transcript, our results suggest that rho is certainly processive enough to reach an elongating transcription complex under these conditions. Our studies of the processivity of translocation under different reaction conditions will be presented elsewhere (K.M.W., J.M.D., and P.H.v.H, in preparation).

Since rho binds cooperatively to the RNA substrates under our reaction conditions, it is possible that single rho hexamers are less processive than multiple rho hexamers. This is suggested by the helicase experiments at 0.2 nM rho hexamers, where only half of the RNA−DNA hybrids that are bound to rho are separated in a single round (Figure 4). If one hexamer falls off the RNA upstream of the RNA−DNA hybrid, a second hexamer could continue to translocate. Alternately, multiple rho hexamers may move more processively than single rho hexamers. In contrast, a single rho hexamer appears to move processively through the 100 bp RNA−DNA hybrid on the blocked helicase substrate (Figure 5). The difference between these two experiments is the distance that rho must travel along single-stranded RNA. It is unknown whether rho binds cooperatively *in vivo*, but estimates of the rho concentration in the cell are in the micromolar range (*10*). At such a high protein concentration, it is likely that rho binds cooperatively to RNA and translocates processively *in vivo*.

Processivity of translocation is a measure of the ability of a protein to traverse a nucleic acid substrate without falling off. Some proteins have evolved special adaptor molecules that allow them to remain bound to a DNA template while translocating along it. For example, the replication complexes of most organisms include a ring-shaped processivity factor that may enclose the DNA substrate and assist the loading and translocation of the replication machinery onto the DNA template (*17*). The β and β' subunits of *E. coli* RNA polymerase may carry a special clamplike structure that helps keep the protein on the DNA template (*18*).

Rho uses a different mechanism to move processively. It carries six RNA binding sites per hexamer, and the RNA substrate wraps around the outside of the hexamer (*19*). In principle, rho needs only to remain bound to the RNA substrate with at least one RNA binding site at all times in

order to translocate processively. An interaction between multiple substrate binding sites may comprise the mechanism whereby rho binds strongly to the nascent RNA transcript and yet moves rapidly along it.

Other DNA helicases are more and less processive than rho under comparable solution conditions. RecBCD, an enzyme complex involved in DNA repair, carries an ATP-dependent DNA−DNA helicase activity and can separate up to 45 kb of double-stranded DNA before dissociating from the substrate (*20*). The Dda helicase of bacteriophage T4, which is associated with DNA replication and recombination functions, acts less processively in that multiple protein binding and release steps are required to separate a ∼300 bp DNA hybrid (*21*). These results, in combination with ours, suggest that the processivity of each helicase may be "tuned" to be appropriate for its function. We have found that the processivity of rho is regulated in part by RNA secondary structure (K.M.W., J.M.D., and P.H.v.H., in preparation). The effect of secondary structure may be more pronounced for RNA helicases than for DNA helicases because much of the RNA in a cell is single-stranded, while DNA is present primarily as long, double-stranded sequences except for the short, transient single-stranded regions that occur at the replication fork.

Processive translocation does not mean that every intervening mucleotide residue must be contacted in turn by a moving rho hexamer. Rho may pass over RNA hairpins in the single-stranded RNA region of the helicase substrate, thus shortening the actual distance traversed along the RNA. Since increasing the secondary structure of the RNA substrate decreases the ATPase activity (*14*) and the translocation rate (K.M.W., unpublished results) of rho, it is possible that movement past these hairpin obstructions could limit the translocation rate of rho.

Effects of the Length of the RNA−DNA Hybrid on Helicase Rates. We performed helicase reactions with RNA−DNA hybrids of different lengths. Hybrids of 20−100 bp were separated at equivalent rates (Figures 3A and 5A). When two DNA oligomers were annealed next to one another, no intermediate products were detected (data not shown), indicating that rho translocates rapidly through an RNA−DNA hybrid that is up to 100 bp in length and that the release of the individual DNA oligomers cannot by resolved. Since rho appears to reach the upstream edge of longer RNA−DNA hybrids more rapidly (Figure 5B), and since all adjacent DNA oligomers are effectively removed together, the DNA_{22} oligomer is removed faster when it is adjacent to a longer RNA−DNA hybrid than when it is annealed to RNA_{255} alone. This suggests that rho may actually translocate faster through an RNA−DNA hybrid than along bare RNA, perhaps because of the absence of RNA secondary structure in these substrates. If DNA oligomers bind to some of the RNA binding sites on rho during the helicase reaction, rho translocation through the RNA−DNA hybrid may be facilitated by rapid dissociation of the DNA oligomers from rho since DNA binds less tightly to rho than does RNA. This postulated faster release of DNA (compared to RNA) may free binding sites on rho that can then move to the next RNA segment.

The amplitude of the helicase reaction increases with the length of the RNA−DNA hybrid (Figures 3A and 5). This is not due to a change in processivity, since rho appears to be totally processive when removing the DNA_{22} oligomer in 50 mM KCl (Table 1). Since the rho binding site size is ∼60−80 nt of RNA (*7*), and since approximately two rho hexamers bind to each RNA, we estimate that rho covers the entire rho loading site of RNA_{255}. This leaves only ∼40−80 nt between rho and the upstream end of DNA_{44}. It is possible that the presence of the DNA_{44} oligomers changes the distribution of rho hexamers so there are fewer rho hexamers per RNA_{255} molecule. This would result in a larger burst amplitude. We confirmed this by showing that the burst amplitude was even larger in the presence of a 100 bp hybrid (Figure 5A).

Our results with different lengths of RNA−DNA hybrid can be compared with the results of others. The rate of a rho helicase reaction with a 340-base RNA molecule containing a 119 bp RNA−DNA hybrid (formed with a single DNA molecule) was ∼75% of the rate with the same RNA molecule containing a 27 bp hybrid (*22*). These reactions were performed in the absence of DNA trapping molecules, and since the binding site size of rho is ∼80 nt (*8*), it is possible that the 5′-end of the RNA−DNA hybrid could rehybridize after rho had translocated part way through it. The translocation rate of rho through a long, continuous RNA−DNA hybrid in the absence of a DNA trap may be slower than the translocation rate along bare RNA or the rate through hybrids formed by multiple, shorter DNA oligomers. Our results clearly demonstrate that rho can separate long RNA−DNA hybrids rapidly in the absence of DNA reannealing. The ATPase activity of rho in the presence of the long RNA−DNA hybrid substrate was not reported in the earlier work (*22*), so the number of ATP molecules consumed per bp traversed in these experiments cannot be calculated.

Stoichiometry of Rho−RNA Binding. We determined the stoichiometry of rho binding to RNA by showing that all of the rho hexamers present are bound to RNA in the helicase reactions, and also by measuring directly the fraction of RNA bound to rho (Table 2 and Results). We found that 2−3 and ∼4 rho hexamers bind to each RNA_{255} and RNA_{391} substrate, respectively. The stoichiometry of rho binding to RNA_{255} increased slightly as the rho concentration increased from 5 to 20 nM rho hexamers (at 10 nM helicase substrate) while the stoichiometry stayed approximately constant for RNA_{391} with 10 or 20 nM rho hexamers at the same substrate concentration (Table 2). This is the first time that the stoichiometry of rho binding to RNA has been determined for natural RNA substrates under helicase reaction conditions. Since there are multiple rho hexamers bound to each RNA substrate, we wanted to know if the stoichiometry would decrease at different RNA or rho concentrations. At RNA and rho hexamer concentrations of 0.2 nM, ∼1.4 rho hexamers bound to each RNA_{255} molecule (see Results). This result suggests that rho binds to the helicase substrates cooperatively.

Previous experiments had shown that rho binds cooperatively to poly(rC). Using both fluorescent binding measurements and an analysis of electron micrographs of rho bound to poly(rC), a cooperativity parameter (ω) of ∼400 and a binding site size of ∼80 nt were determined for rho hexamers (*7*, *8*). This moderate cooperativity parameter predicts that the average cluster size of rho hexamers on RNA should be 2 when the RNA is 30% saturated by rho. We estimated the binding density of rho on the RNA in our experiments by assuming that each rho hexamer covers ∼80 nt. An

average stoichiometry of 2−3 rho hexamers was observed when 16−62% of the RNA_{255} was bound to rho, and an average stoichiometry of 4 hexamers was observed when 21−41% of the RNA_{391} was bound to rho (Table 2). Our results indicate that the cooperativity of rho binding is slightly higher on RNA_{391} than on poly(rC), suggesting that the apparent cooperativity may depend somewhat on the RNA substrate, but this effect is not large.

We have used nitrocellulose filter-binding data to estimate the fraction of RNA bound to rho (Table 2). Since rho translocates processively under these reaction conditions, the fraction of RNA bound to rho and the fraction of DNA oligomers removed in the first round of the helicase reaction are similar (Table 1). In the experiments with either RNA_{255} or RNA_{391} at a 2:1 rho hexamer to RNA ratio, we found that the burst amplitude was slightly higher than the fraction of RNA bound to rho under the same conditions (Table 1). The difference in the two values is smaller than the error in the filter-binding measurements, and we did not observe a difference in binding at 37 °C compared to 22 °C (data not shown). If we use the burst amplitude to estimate the fraction of RNA molecules bound to 20 nM rho in Table 2, we calculate a slightly smaller number of rho hexamers per RNA molecule. We therefore consider the stoichiometry estimates of Table 2 to represent an upper limit.

Model for the ATP-Dependent Translocation of the Rho Hexamer along RNA. The cooperative binding of rho to RNA in our experiments has implications for models of the rho translocation process. One model that has been considered is a "simple tracking" model, in which the rho hexamer binds to RNA at the rho loading site and translocates downstream by releasing and rebinding RNA sequences sequentially (*19*, *23*). A second model that has been described is called "tethered tracking". In this model, it is proposed that rho remains bound to the RNA of the rho loading site through some of its RNA binding sites, and that it utilizes the others to translocate (*24*, *25*). This model predicts that rho would remain bound to the rho loading site even after translocating to the 3′-end of the RNA substrate.

We have shown here that multiple equivalent rho hexamers are bound to each RNA molecule, and that neighboring hexamers may translocate behind the first hexamer. Upstream hexamers could remain bound to the RNA near the rho loading site if the RNA substrate is too short to allow multiple hexamers to bind downstream (on the 3′ side) of the rho loading site. This means that the previous experiments (*24*, *25*) supporting the tethered-tracking model must be reevaluated, since the analyses assumed only one rho hexamer to be bound per RNA molecule and the experiments were performed under reaction conditions similar to those used here (i.e., where rho binds cooperatively to the RNA).

Previous studies of rho-dependent termination have suggested that one rho hexamer per nascent RNA is sufficient to cause termination (*26*, *27*). Rho-dependent termination sites usually occur within ∼100 nt after the rho loading site on the RNA has been transcribed. The first rho-dependent termination sites studied in detail were those of the λ t_{R1} terminator, which is located downstream of the λ P_R promoter. The rho loading site on the *cro* RNA transcribed from this gene lies between transcript positions 225 and 280 (positions are numbered from the P_R promoter) (*15*, *28*), and the rho-dependent termination sites occur between positions 290 and 450 (*29*−*31*). Using a minimal substrate that does not contain the entire *cro* coding region, Hart and Roberts (*26*) showed that rho could terminate transcripts in rC-rich regions after only 85 nt had been transcribed. This is consistent with results with the *trp t′* rho-dependent termination system, for which a rho loading site ∼105 bp in length is sufficient to cause termination (*27*, *32*). This conclusion has also been confirmed by results from our laboratory, which show that the *trp t′* rho loading site is capable of causing termination after 80−90 nt have been transcribed (A. Q. Zhu and P. H. von Hippel, manuscript in preparation). Since the binding site size for the rho hexamer on poly(rC) is ∼70 nt (*7*, *8*), these results confirm that one fully-bound rho hexamer can trigger termination, since the minimum size of the nascent RNA that can be terminated is comparable to the binding site size for one rho hexamer.

We have asked whether one rho hexamer is sufficient to separate the RNA−DNA hybrids in the helicase reaction. To approach this question, we blocked the RNA_{255} substrate on either end by annealing DNA oligomers, leaving only ∼150 nt of single-stranded RNA. When we performed helicase reactions with these substrates, we found that the burst amplitude was larger than the amplitude with the RNA_{255}/DNA_{22} substrate to which rho binds cooperatively, suggesting that fewer rho hexamers are bound to each partially blocked substrate (Figure 5). We also found that the ATPase activity of rho in the presence of the partially blocked substrate containing a free rho loading site was similar to that for the other RNA_{255} substrates. All of these results indicate that the properties of each rho hexamer on the RNA substrate are similar, and that one rho hexamer is sufficient to separate RNA−DNA hybrids that are up to 100 bp in length. However, a single rho hexamer does not appear to be able to translocate totally processively along the single-stranded RNA because at 0.2 nM concentrations of rho hexamers and RNA_{255}, only half of the bound RNA substrates have a DNA oligomer removed in the first round of the helicase reaction (Figure 4).

ATPase Activity during the Helicase and Translocation Reactions. We observed that the ATPase activity of RNA-bound rho is constant, even when the concomitant helicase reactions show variable helicase activity (Figure 2). We measured the RNA-dependent ATPase activity of rho in the presence of RNA_{255} annealed to five different DNA oligomers to form RNA−DNA hybrids varying from 20 to 100 bp in length, or with "bare" RNA devoid of any RNA−DNA hybrid (see Figure 3B and Results). The ATPase rate in the presence of all of these substrates is similar (Figure 3 and Results). Since the presence of RNA−DNA hybrids does not significantly perturb the rho−ATPase activity, this shows that rho hydrolyzes approximately as much ATP per nucleotide residue traversed in simple translocation as it does while separating RNA−DNA hybrids. This finding, in turn, means that moving through RNA−DNA hybrids neither inhibits the ATPase activity of rho (perhaps by slowing down translocation) nor stimulates it (perhaps by causing rho to expend more free energy per unit time in separating the RNA−DNA hybrid than is expended in simple translocation). In fact, since rho appears to translocate faster through the RNA−DNA hybrid than along single-stranded RNA (Figure 5), rho may consume less ATP per RNA residue traversed during the hybrid separation step of the helicase reaction. We conclude that the RNA binding and release

cycle of rho that is driven by ATP hydrolysis is essentially "decoupled" from the actual helicase activity of this protein.

Our results demonstrate that the RNA component is indeed the main ATPase cofactor in the helicase reaction, and that the presence of DNA oligomers in the reaction has no significant effect, whether they are annealed to the RNA or not. This is consistent with what is known about the properties of rho. Previous experiments with the *cro* transcript of phage λ showed that the rho loading site of this transcript is the main activator of rho ATPase activity (*15*). Since most of the DNA oligomers used for the helicase reactions do not anneal to the rho loading site, it is reasonable that they do not affect the initial rho−RNA interaction. This is confirmed by the nitrocellulose filter-binding measurements, which showed no effect of DNA oligomers on rho−RNA binding (see Results). However, we know that rho removes the DNA oligomers annealed to the RNA, so rho must eventually reach the 3′ end of the RNA molecule. This indicates that as long as rho can bind initially to the rho loading site, the presence of DNA oligomers annealed to the RNA that are reached by translocation along the RNA does not affect the observed ATPase activity.

It appears that the main function of rho is to translocate along RNA, and that it removes hybridized DNA oligomers from the RNA as a "by-product" of this reaction. This is similar to a reaction carried out by the poliovirus RNA-dependent RNA polymerase. This protein synthesizes RNA from the poliovirus RNA genome, but it can also synthesize RNA from an RNA substrate that is hybridized to an antisense RNA. Carrying out the RNA synthesis reaction in the presence of the antisense RNA does not require excess ATP hydrolysis and does not slow down RNA synthesis (*33*). As a consequence, these workers have called the poliovirus RNA polymerase an RNA unwindase instead of a helicase because it did not appear to consume additional ATP in unwinding the RNA−RNA hybrid. This may be a more appropriate name for the comparable activity carried out by rho since, as we have shown, rho also does not hydrolyze extra ATP in separating RNA−DNA hybrids.

There is considerable evidence that the elongation complex of *E. coli* RNA polymerase contains an RNA−DNA hybrid that is 8−12 bp in length, and this conclusion is consistent with the results of most recent mechanistic transcription studies (*34*). It is possible that the transcription termination function of rho consists primarily of separating this hybrid. However, it is not known whether the hybrid within the transcription complex is "covered" by RNA polymerase or whether it lies on the surface of the complex. Thus, rho could act by "pulling" the RNA out of the elongation complex, or it may "activate" the RNA polymerase to release the transcript in some other way. It has been suggested that the RNA polymerase dissociates from the DNA template at about the same time as the RNA transcript is released in rho-dependent termination (*35*). If rho can totally disrupt the transcription complex, it must be a powerful "molecular motor" in its own right, since RNA polymerase exerts more force in moving along DNA than do cytoskeletal motors in moving along tubulin or actin (*36*). Therefore, rho either must exert a greater force in disrupting the RNA polymerase complex or must induce a destabilizing conformational change in the RNA polymerase complex. Alternatively, rho may only be able to bring about termination if the elongation complex is already destabilized in some way, perhaps as a consequence of reaching pause sites along the template (A. Q. Zhu, unpublished results).

ATP Consumption. We estimate that rho hydrolyzes 1−2 ATP molecules per nucleotide residue traversed while translocating along RNA_{255} and RNA_{391} (Table 2). Previously, Brennan et al. (*2*) determined that rho hydrolyzed ∼4000 molecules of ATP per 28 bp RNA−DNA hybrid separated from a ∼250 nt RNA substrate containing the same *trp t′* rho loading site that we have used. Based on our estimate that rho translocates over ∼100 nt on this substrate, these results would indicate that rho hydrolyzes ∼40 ATP molecules per nucleotide residue traversed during the translocation reaction. The differences in the ATP consumption rates observed in these experiments arise because our helicase rate is ∼14-fold higher than that estimated by the earlier workers. This difference is a result of the different ways the helicase analyses were conducted in the two studies. Thus, our first time points were obtained 10 s after the reaction was initiated, while in the previous work 30 s time points were used to calculate the initial rates. Since the first phase of the helicase reaction is essentially over in 10−20 s, a 30 s measurement will significantly underestimate the actual initial rate. This can account for the differences in rho-dependent helicase rates and ATP consumption rates reported in the two studies.

The ATP consumption rate of rho can be compared with that determined for the RecBCD protein, which is the only other helicase for which this calculation has been made. The rate of ATP hydrolysis for this enzyme is 2−3 ATP molecules consumed per bp unwound (*6*). This is similar to the ATP consumption rate that we have measured for rho. Therefore, although RecBCD translocates 50 times faster than rho (see above), they both hydrolyze similar amounts of ATP per residue traversed. The hydrolysis of one ATP molecule yields enough free energy to separate 2−4 bp of double-stranded DNA (*6*); thus, both enzymes utilize the free energy of ATP hydrolysis with reasonable efficiency.

It has been found with DNA helicases (especially the *rep* helicase, see reference *37*) that the ATPase activity depends on the oligomeric state of the enzyme and on the type of substrate bound to it. This finding shows that determination of the ATP consumption rate for a helicase can be complicated. The situation is simpler for rho because it exhibits very little ATPase activity unless all of its binding sites are filled with RNA (Y. Wang and P. H. von Hippel, in preparation). This indicates that in our experiments only rho hexamers with all of their RNA binding sites bound to RNA should hydrolyze ATP at a significant rate. For these reasons, our calculations of the rate of ATP consumption by rho should be accurate.

Model for the Translocation Reaction. The ATP consumption rate of rho has implications for the mechanism of translocation along RNA. A physical model for rho translocation has been proposed (*19*). In this model, translocation is dependent on two features of the RNA−rho complex. These are the following: (i) the fact that each asymmetric dimer of the rho hexamer contains a strong and a weak binding site for both RNA and ATP; (ii) the fact that RNA is released by ATP hydrolysis, which triggers a conformational change that "switches" the affinities of the RNA binding sites within the rho dimer. The model of Geiselmann et al. (*19*) predicts that when ATP is hydrolyzed, RNA bound to the previously strong binding site of the rho dimer is

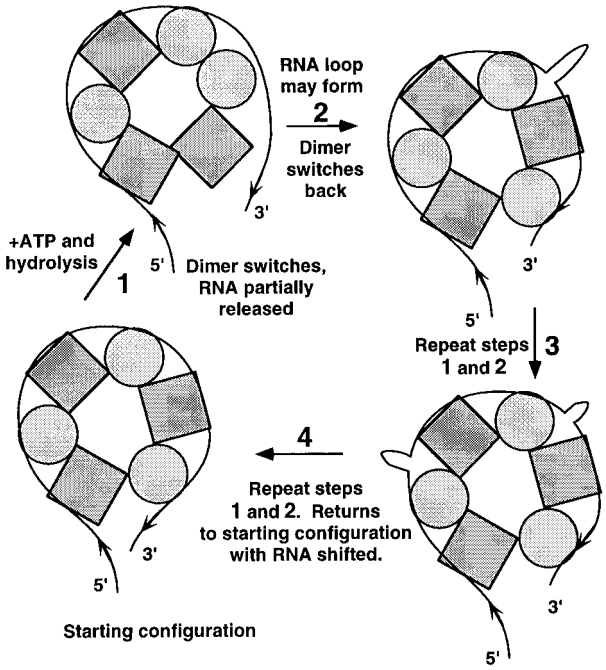

FIGURE 6: Model for the translocation of rho along RNA. This figure shows a model of how RNA might move along the surface of rho during the translocation reaction. The circles and squares represent rho monomers in two different conformations. Each asymmetric dimer carries one strong and one weak RNA and one strong and one weak ATP binding site. Upon ATP hydrolysis, the conformations of the subunits switch, and RNA is released. The probability of the loop being "injected" from the 3′ side is always higher because of chain asymmetry with respect to "end" dimers. The loops may contain RNA hairpins. Movement is a stochastic process, corresponding to a biased random walk in the 3′ direction. On average, each hexamer traverses 0.5−1 nt per ATP hydrolysis (and RNA chain release) event.

released, and that these sites can bind RNA anew after another round of ATP hydrolysis. The site size for RNA binding on a rho subunit is ∼11 nt, but the actual RNA binding site interacts with ∼8 nt of RNA (*38*). This means that there are ∼3 nt between each RNA binding site. If one ATP hydrolysis event is sufficient to release the RNA from a rho dimer (see reference *19*), then we might expect that the rate of ATP consumption for rho might be as low as 1 ATP molecule consumed per 22 nt of RNA traversed. We have measured here a rate that is 20−40-fold higher. This suggests that even if one ATP hydrolysis event does release 22 nt of RNA from a rho dimer, on average the distance translocated along the RNA as a consequence is less than 1 nt per rho dimer binding and release cycle. This modified version of the Geiselmann et al. model is outlined in Figure 6.

This model of the rho translocation process is consistent with our finding that the ATPase activity of rho is the same whether rho is translocating along RNA in the burst phase of the helicase reaction or is bound to the 3′-end of the RNA component of the helicase substrate (Figure 3A). In the latter position, according to our model (Figure 6), rho would simply rebind the RNA that it has just released; i.e., it "marches in place." In addition, the ATPase rate is independent of the length of the RNA−DNA hybrid on the helicase substrate. These results indicate that the ATPase activity of rho is not tightly coupled to translocation and that our estimates of the ATP consumption rate of rho represent an upper limit. It is likely that the ATPase activity of rho is coupled to the rate of RNA release at each individual RNA binding site of the rho hexamer. It is interesting to note that rho may translocate through an RNA−DNA hybrid somewhat more rapidly than it moves along single-stranded RNA. This indicates that RNA loop translocation (see Figure 6) may be more effective when rho is moving through an RNA−DNA hybrid, since here translocation is not perturbed by preexisting RNA secondary structure.

In a different model describing rho−RNA binding, it has been suggested that the RNA chain binds to one face of the rho hexamer and then passes through the hole in the center (*39*). We showed in the previous paper that rho acts as a catalytic helicase in reaction buffer containing 150 mM KCl (*3*). In experiments described elsewhere (K.M.W., J.M.D., and P.H.v.H., manuscript in preparation), we found that rho does not move along the RNA with full processivity under these conditions. This suggests that rho does not have to reach the end of the RNA molecule in order to fall off, and this result is not consistent with a model in which RNA must pass through the center of the rho hexamer.

Direction of Translocation. We have shown that rho translocates >3000-fold faster in the 5′ → 3′ direction compared to the 3′ → 5′ direction (*3*). Since the different states of rho during the translocation reaction shown in Figure 6 are thermodynamically similar, the direction of translocation must be a result of kinetic factors. In our model (*19*, and Figure 6), the RNA chain enters and exits the rho hexamer between two asymmetric dimers and is only bound to rho on one side of these dimers. This increases the probablility that RNA will be released first from these dimers when ATP is hydrolyzed. Previous experiments have also shown that the ATPase activity of rho depends on the polarity of rU and rC residues in the RNA segment bound to each RNA binding site (*38*) and that this dependence is not a result of altered RNA binding affinity (*40*). These results suggest that the polarity of the RNA chain bound to each dimer may bias the movement of rho along RNA in the 5′ → 3′ direction.

ACKNOWLEDGMENT

We thank members of our laboratory for helpful discussions and the reviewers for insightful comments.

REFERENCES

1. Brennan, C. A., Dombroski, A. J., and Platt, T. (1987) *Cell 48*, 945−952.
2. Brennan, C. A., Steinmetz, E. J., Spear, P., and Platt, T. (1990) *J. Biol. Chem. 265*, 5440−5447.
3. Walstrom, K. M., Dozono, J. M., Robic, S., and von Hippel, P. H. (1997) *Biochemistry* (preceding paper in this issue).
4. Lohman, T. M., and Bjornson, K. P. (1996) *Annu. Rev. Biochem. 65*, 169−214.
5. Coy, D. L., and Howard, J. (1994) *Curr. Opin. Neurobiol. 4*, 662−667.
6. Roman, L. J., and Kowalczykowski, S. C. (1989) *Biochemistry 28*, 2873−2881.
7. McSwiggen, J. A., Bear, D. G., and von Hippel, P. H. (1988) *J. Mol. Biol. 199*, 609−622.
8. Bear, D. G., Hicks, P. S., Escudero, K. W., Andrews, C. L., McSwiggen, J. A., and von Hippel, P. H. (1988) *J. Mol. Biol. 199*, 623−635.
9. Finger, L. R., and Richardson, J. P. (1982) *J. Mol. Biol. 156*, 203−219.
10. Geiselmann, J., Yager, T. D., Gill, S. C., Calmettes, P., and von Hippel, P. H. (1992) *Biochemistry 31*, 111−121.
11. Geiselmann, J., Seifried, S. E., Yager, T. D., Liang, C., and von Hippel, P. H. (1992) *Biochemistry 31*, 121−132.

12. McGhee, J. D., and von Hippel, P. H. (1974) *J. Mol. Biol. 86*, 469−489.
13. Cashel, M., Lazzarini, R. A., and Kalbacher, B. (1969) *J. Chromatogr. 40*, 103−109.
14. Richardson, J. P., and Macy, M. R. (1981) *Biochemistry 20*, 1133−1139.
15. Faus, I., and Richardson, J. P. (1989) *Biochemistry 28*, 3510−3517.
16. Nehrke, K. W., and Platt, T. (1994) *J. Mol. Biol. 243*, 830−839.
17. Reddy, M. K., Weitzel, S. E., and von-Hippel, P. H. (1993) *Proc. Natl. Acad. Sci. U.S.A. 90*, 3211−3215.
18. Nudler, E., Avetissova, E., Markovtsov, V., and Goldfarb, A. (1996) *Science 273*, 211−217.
19. Geiselmann, J., Wang, Y., Seifried, S. E., and von Hippel, P. H. (1993) *Proc. Natl. Acad. Sci. U.S.A. 90*, 7754−7758.
20. Roman, L. J., and Kowalczykowski, S. C. (1989) *Biochemistry 28*, 2863−2873.
21. Jongeneel, C. V., Formosa, T., and Alberts, B. M. (1984) *J. Biol. Chem. 259*, 12925−12932.
22. Steinmetz, E. J., Brennan, C. A., and Platt, T. (1990) *J. Biol. Chem. 265*, 18408−18413.
23. Platt, T. (1994) *Mol. Microbiol. 11*, 983−990.
24. Faus, I., and Richardson, J. P. (1990) *J. Mol. Biol. 212*, 53−66.
25. Steinmetz, E. J., and Platt, T. (1994) *Proc. Natl. Acad. Sci. U.S.A. 91*, 1401−1405.
26. Hart, C. M., and Roberts, J. W. (1994) *J. Mol. Biol. 237*, 255−265.
27. Galloway, J. L., and Platt, T. (1988) *J. Biol. Chem. 263*, 1761−1767.
28. Chen, C.-Y. A., and Richardson, J. P. (1987) *J. Biol. Chem. 262*, 11292−11299.
29. Lau, L. F., Roberts, J. W., and Wu, R. (1983) *J. Biol. Chem. 258*, 9391−9397.
30. Morgan, W. D., Bear, D. G., and von Hippel, P. H. (1983) *J. Biol. Chem. 258*, 9553−9564.
31. Ceruzzi, M. A. F., Bektesh, S. L., and Richardson, J. P. (1985) *J. Biol. Chem. 260*, 9412−9418.
32. Zalatan, F., Galloway-Salvo, J., and Platt, T. (1993) *J. Biol. Chem. 268*, 17051−17056.
33. Cho, M. W., Richards, O. C., Dmitrieva, T. M., Agol, V., and Ehrenfeld, E. (1993) *J. Virol. 67*, 3010−3018.
34. Nudler, E., Mustaev, A., Lukhtanov, E., and Goldfarb, A. (1997) *Cell 89*, 33−41.
35. Andrews, C., and Richardson, J. P. (1985) *J. Biol. Chem. 260*, 5826−5831.
36. Yin, H., Wang, M. D., Svoboda, K., Landick, R., Block, S. M., and Gelles, J. (1995) *Science 270*, 1653−1657.
37. Wong, I., Moore, K. J., Bjornson, K. P., Hsieh, J., and Lohman, T. M. (1996) *Biochemistry 35*, 5726−5734.
38. Wang, Y., and von Hippel, P. H. (1993) *J. Biol. Chem. 268*, 13940−13946.
39. Richardson, J. P. (1996) *J. Biol. Chem. 271*, 1251−1254.
40. Wang, Y., and von Hippel, P. H. (1993) *J. Biol. Chem. 268*, 13947−13955.

BI963180R